GEOCHEMICAL AND PETROLOGICAL CHARACTERISTICS OF LATE TRIASSIC BASIC VOLCANIC ROCKS FROM THE KOCALI COMPLEX, SE TURKEY: IMPLICATIONS FOR THE TRIASSIC EVOLUTION OF SOUTHERN TETHYS

Elif Varol*,✉, Yavuz Bedi, Ugur Kagan Tekin*** and **Seda Uzuncimen***

** Geological Engineering Department, Hacettepe University, Ankara, Turkey.*
*** General Directorate of Mineral Research and Exploration, Geological Research Department, Ankara, Turkey.*
✉ *Corresponding author, e-mail: elvarol@hacettepe.edu.tr*

Keywords: *Basic volcanics, petrology, geochemistry, E-MORB, OIB, Late Triassic, radiolarian dating, the Kocali Complex, Southern Tethys. SE Turkey.*

ABSTRACT

The Kocali Complex in SE Anatolia is mainly composed of tectonically imbricated slices of pelagic rock suits (pelagic limestones, cherts, etc), platform carbonates, clastics, serpentinites and basic volcanics. It can be subdivided into four main parts as the Tarasa Unit, the Konak Unit, the Cilo Limestones and the Kale Ophiolite. In this paper, geochemical characteristics of basic volcanic rocks associated with pelagic sediments (radiolarian cherts, pelagic limestones, etc) have been studied along four stratigraphical sections (the Tarasa, the Bulam-2, the Korun-1 and the Korun-2) in the Konak and the Tarasa Units. The age of the volcanic sequences have been assigned to Late Triassic (middle Carnian to Rhaetian) based on the radiolarian data from the associated pelagic rock units.

Geochemical data indicates the presence of two different types of Late Triassic volcanic rock groups characterized by E-MORB-type (Group-1 volcanites from the Tarasa Unit formed by mixing of OIB and MORB-type melts) and OIB-type (Group-2 volcanites from the Konak Unit) mantle sources. None of the samples from the Kocali Complex has characteristics of N-MORB type mantle source and was affected by crustal contamination. Based on these data, it can be suggested that all these volcanic rocks formed in a marginal oceanic basin away from the ocean ridge. The presence of Radiolaria and Bivalvia-bearing pelagic limestones and cherts associated to the basic volcanic rocks in the Kocali Complex also emphasize that they all formed in deep marine basin.

Geochemical characteristics of Late Triassic volcanics in the Kocali Complex have great similarities and well-correlative to the coeval volcanics previously studied in the Southern Tethyan Belt (e.g. the Baer-Bassit region in NW Syria, the Mamonia Complex in SW Cyprus and the Antalya Nappes in SW Turkey). Taking into the consideration of the geochemical data obtained from Late Triassic basic volcanics in the Kocali Complex and geochemical characteristics of the coeval volcanics in the adjacent units in the Southern Tethyan Belt, it can be suggested that rifting age of the Southern Tethyan Oceanic Basin in SE Anatolia is probably earlier than early Late Triassic (middle Carnian time).

INTRODUCTION

The Hawasina basin corresponding to the eastern part as Southern Tethyan passive continental margin can be traced along Pichakun-Pindos Trough to the west (Ricou, 1971; Dumont et al., 1972; Ricou and Marcoux, 1980; Argyriadis et al., 1980; Robertson and Woodcock, 1982; Kazmin et al., 1986; Bechenec et al., 1988; Bernoulli et al., 1990; Fig. 1). In particular, pelagic sedimentation, mainly characterized by radiolarian cherts and pelagic limestones associated with basic volcanics in Permian to Mesozoic time span, has been recorded along this zone in the Hawasina Basin, northeast Oman, the Pichakun Zone and Kermenshah regions in western Iran, the Kocali Complex and the Antalya Nappes in southern Turkey, the Baer-Bassit region in northwest Syria, the Mamonia Complex in southern Cyprus, the Pindos Zone in southern Greece and the Lagonegro Basin in Southern Italy (Kazmin et al., 1986; Bernoulli et al., 1990).

Although stratigraphical properties and ages of pelagic sediments, and geochemistry of the basic volcanic rocks belonging to different parts of this zone have been studied in detail by several authors (e.g. Bernoulli and Weissert, 1987; Bechenec et al., 1988; 1990; De Wever et al., 1988; 1990; Bernoulli et al., 1990; Maury et al., 2003; Lapierre et al., 2004 in the Hawasina basin, Oman. Ricou, 1971; 1976; Robin et al., 2010 in the Pichakun zone, Iran. Gharib, 2009; Gharib and De Wever, 2009 in the Kermenshah region, Iran. Delaune-Mayere, 1984; Al-Riyami et al., 2000; 2002 in the Baer-Bassit region, Syria. Lapierre, 1975; Robertson and Woodcock, 1979; Bragin et al., 2000; Bragin, 2007 in the Mamonia Complex, Cyprus. Dumont et al., 1972; Senel et al., 1992; Tekin, 1999; 2002a; 2002b; Tekin and Yurtsever, 2003; Yurtsever et al., 2003; Varol et al., 2007; Moix et al., 2009 in the Antalya Nappes, Turkey. Fleury, 1980; Danelian et al., 2001 in the Pindos Zone, Greece. Bazzucchi et al., 2005; Bertinelli et al., 2005 in the Lagonegro Basin, Italy), very few studies have been performed on the Kocali Complex, SE Turkey (Sungurlu, 1973; Perincek, 1979a, 1979b).

Bingol (1994) studied the geochemical and petrographical characteristics of the volcanic rocks from the Kocali Complex and reported the differences (e.g. within PB, IAT and Enriched-Mid-Ocean Ridge Basalt) in their geochemical characteristics.

To clarify these differences and to interpret the tectonomagmatic meaning of these volcanic rock samples were obtained along four stratigraphic sections at the north and northeast of Adiyaman, SE Turkey. Dating of these volcanic rocks had been previously achieved by using radiolarian faunas taken from the associated pelagic sediments (Uzuncimen et al., 2009; 2011; Tekin et al., 2010).

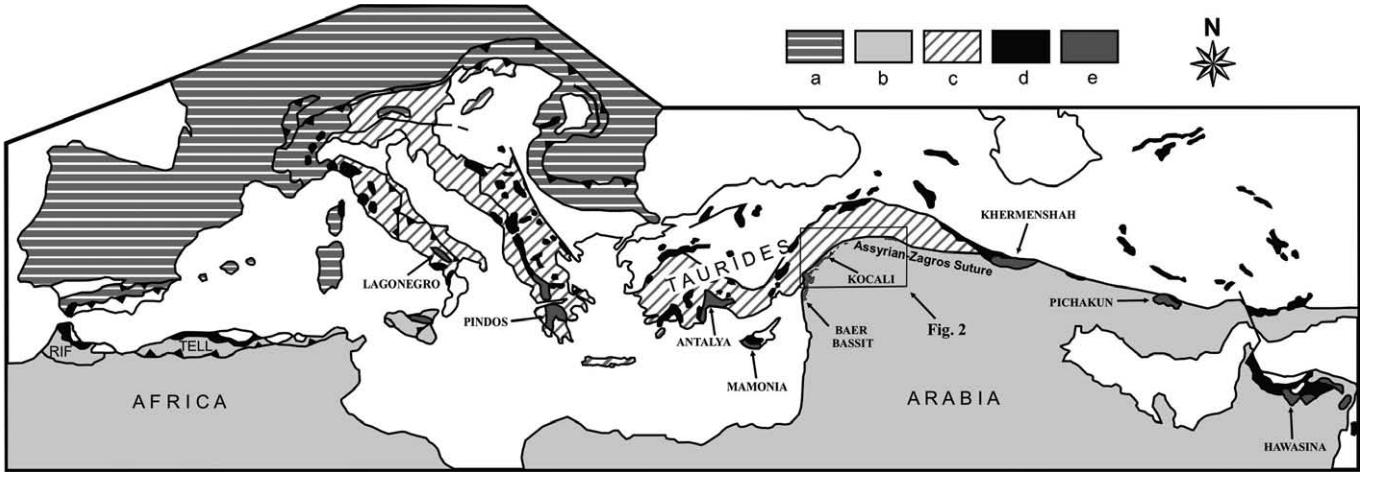

Fig. 1 - Distribution of the remnants of the South Tethyan seaway; a) Eurasia and its continental margins, b) Africa-Arabia and its continental margins, c) Adria, d) Ophiolites and associated oceanic sediments, e) Sclafani-Lagonegro-Pindos-Pichakun-Hawasina South Tethyan Seaway (revised after Ricou and Marcoux, 1980; Bernoulli et al., 1990). Location of Fig. 2 is shown in the map.

GEOLOGICAL SETTING

The Taurus Mountain chain in SE Anatolia with remnants of Tethyan seaways and has a complex geological history (Sengor and Yilmaz, 1981; Goncuoglu et al., 1997; Robertson et al., 2007). Evolution of the most prominent Tethyan seaway (southern Neotethyan seaway) in this area began with rifting in the Triassic and terminated with continent-continent collision in the Miocene (Sengor and Yilmaz, 1981; Robertson et al. 2007). The resulting Bitlis-Zagros Orogen (Sengor and Kidd, 1979; Sengor and Yilmaz, 1981) was formed during this collision, and the remnants of the Tethyan Ocean is marked by the SE Anatolian Suture Belt (Goncuoglu et al., 1997) or the Assyrian-Zagros Suture in SE Anatolia (Okay and Tuysuz, 1999).

Three tectonic zones (the Arabian Platform, an Imbricated Zone, and a Nappe Zone) are recognised in the SE Anatolian Suture Belt according to Yilmaz and Yigitbas (1990), Yilmaz (1993), and Elmas and Yilmaz (2003). On the other hand, according to Senel (2002), two main distinct structural units are present in the region, the Southeast Anatolian Autochthon (corresponding to the Arabian Platform) and the nappes (Fig. 2). The nappes thrusting over the Southeast Anatolian Autochthon can be grouped into three main packages as the Bitlis-Poturge-Malatya Nappes, the Cungus-Hakkari Nappe, and the Kocali-Karadut Nappes. The Kocali-Karadut Nappes within this system constitute the lowermost unit and include different allochthonous units such as the Kocali Complex, the Karadut Complex, the Cilo Limestones, and the Hatay Ophiolites (Senel, 2002).

The Kocali Complex in the Kocali-Karadut Nappes is composed of tectonically imbricated slices of pelagic rock suits (pelagic limestones, cherts etc), platform carbonates, clastics, serpentinites and basic volcanics (Sungurlu, 1973;

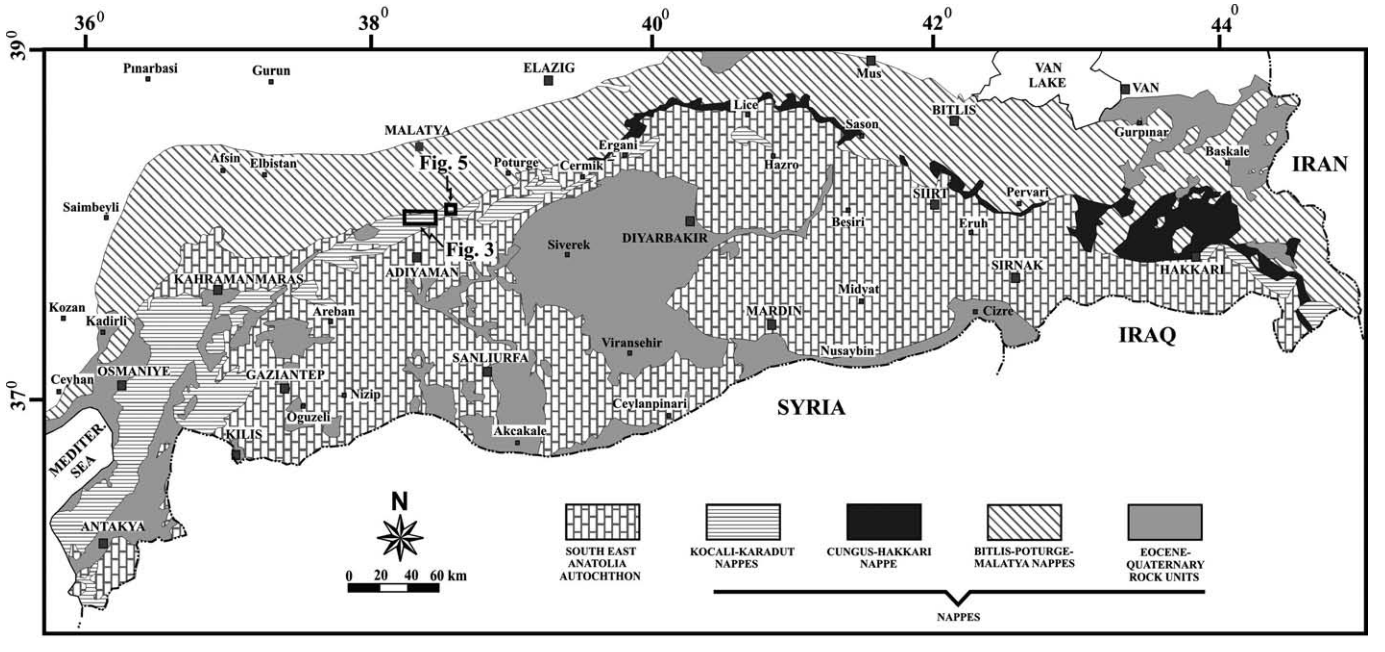

Fig. 2 - Geological map of the SE Anatolia showing the main tectonic units (simplified and revised after Senel, 2002) and studied areas.

Perincek, 1979a; 1979b, 1990). It was initially described by Sungurlu (1973) at the north of Adiyaman where the best outcrops of this complex is exposed (Figs. 1 and 2). As a remnant of Southern Tethyan seaway (Kazmin et al., 1986; Bernoulli et al., 1990) or Southern Neotethys, rock-units of the Kocali Complex are traced along the Assyrian-Zagros Suture Zone from the southeastern border of Turkey to the Mediterranean Sea (Figs. 1 and 2). In the type locality, Sungurlu (1973) subdivided the complex into three lithological associations: volcanics, sedimentary units and ultrabasics. Late Jurassic - Early Cretaceous fossil findings (benthonic foraminifera and calpionellids) have been reported from the limestones in the sedimentary units. Subsequently, in Adiyaman region, this complex was subdivided into the Tarasa, Konak, and Kale Formations by Perincek (1978; 1979a; 1979b). According to this author, the Tarasa Formation, corresponding to the volcanic unit of Sungurlu (1973), is composed of basalts, spilitic basalts, and diabase with a total thickness of 400-1000 m. The Konak Formation, up to 1800 m thick, comprises limestones, radiolarites, volcanic rocks and silicified shales, and corresponds to the sedimentary units of Sungurlu (1973). Moreover, the Kale Formation, as the uppermost tectonic unit of the Kocali Complex, corresponds to the ultrabasics of Sungurlu (1973) and includes serpentinites, diorites, diabases, and gabbros.

Further east in the Hakkari region, this complex was also subdivided into three sedimentary units (the Kirmizitas and Yesiltas Formations, and the Cilo Limestones) (Perincek, 1990). Here, the Kirmizitas Formation of Jurassic age based on algae flora, is composed of lavas, basic tuffs, diabases, pelagic limestones, and radiolarites. It is the equivalent of the Konak Formation in the Adiyaman region. The Cilo Limestones include massive limestones and marbles and its age were assigned to Late Triassic to presumed Jurassic age based on megalodont fauna. The uppermost tectonic unit of the Kocali Complex in Hakkari region is the Yesiltas Formation including ophiolitic rock units. According to Perincek (1990) its age is presumably Late Triassic - Early Cretaceous and it is the equivalent of the Kale Formation in the Adiyaman region. In this study, we adopted the names: the Tarasa Unit for the Tarasa Formation, the Konak Unit for the Konak Formation and the Kale Ophiolite for the Kale Formation, as all these units are individual tectonic slices with different rock-units, rather than lithostratigraphic entities.

GENERAL CHARACTERISTICS AND AGE OF THE STRATIGRAPHIC SECTIONS

Geochemical and petrographical characteristics of the studied basic volcanics were obtained from four stratigraphic sections, the Bulam-2, the Tarasa, the Korun-1 and the Korun-2. While the Bulam-2, the Korun-1 and the Korun-2 sections have been studied within the Konak Unit, the Tarasa section has been measured from the rock units of the Tarasa Unit.

The Bulam-2 and the Tarasa sections are located around the Bulam Creek at the north of Adiyaman (Figs. 2, 3 and Table 1). The Bulam-2 section, 160 m thick, is exposed at the northern bank of Bulam Creek and succession of the Bulam-2 stratigraphic section is overturned due to Miocene compressional tectonics. Due to this, both Bolkardag Metamorphics of the Bitlis-Poturge-Malatya Nappes and the overlying volcano-sedimentary Maden Complex of Eocene

Table 1 - Coordinates for localities discussed in text, given in UTM (Universal Transverse Mercator).

Section	Coordinates	Map
The Bulam-2 section	Base: 4204630 North / 436871 East	Sanliurfa M40-b1
	Top: 4204518 North / 436820 East ZONE 35T	
The Korun-1 section	Base: 4206072 North / 457359 East	Malatya L41-d4
	Top: 4206340 North /457151 East ZONE 35T	
The Korun-2 section	Base: 4206340 North / 457151 East	Malatya L41-d4
	Top: 4206626 North / 457198 East ZONE 35T	
The Tarasa section	Base: 4203582 North / 443323 East	Sanliurfa M40-b1
	Top: 4202947 North / 443193 East ZONE 35T	
Additional samples around the Tarasa section	**Coordinates**	**Map**
TAR-1-29	4203500 North / 443032 East	Sanliurfa M40-b1
TAR-1-34	4203210 North / 442772 East	Sanliurfa M40-b1
TAR-1-36	4203130 North / 442857 East	Sanliurfa M40-b1
TAR-1-38	4203020 North / 443000 East	Sanliurfa M40-b1
TAR-1-40	4203611 North / 443804 East	Sanliurfa M40-b1
TAR-1-41	4203612 North / 443504 East	Sanliurfa M40-b1

age (Perincek, 1978) were thrust over the Kocali Complex (Fig. 3). The basal part of the Bulam-2 section is dominated with green basic volcanics with rare cherts and silicified mudstone breaks (Fig. 4). Higher in the section, gray to beige, thin to medium-bedded, Radiolaria and Bivalvia bearing limestones with chert nodules and an alternation of gray to beige, thin to medium-bedded limestones and green to red, thin-bedded chert are dominant lithologies (Fig. 4). Limestones, sandstones and cherts interbedded within the basic volcanic rocks characterize the upper part of the section. From twenty-two volcanic rock and pelagic sediment samples collected along this section, only three least-altered samples (Bul-2-7, Bul-2-11, Bul-2-22) were used for geochemical analyses and five samples (Bul-2-3, Bul-2-6, Bul-2-10, Bul-2-19 and Bul-2-20) are productive for Radiolaria determinations and dating. Detailed studies performed on the radiolarians of this section reveal that the age of the basal part of the section (sample Bul-2-3) is early middle Carnian. Towards the upper part of the section, latest Carnian/earliest Norian to early Norian age for the sample Bul-2-6, middle to late Norian age for the sample Bul-2-10, late Norian age for the samples Bul-2-19 and Bul-2-20 have been assigned. Based on these data, it is concluded that succession in the Bulam-2 section has been deposited during early middle Carnian - late Norian time span (Uzuncimen et al., 2009; 2011; Tekin et al., 2010).

Widespread basic volcanic rocks are exposed at the valley of Tarasa Creek, to the east of the Bulam-2 section (Fig. 3 and Table 1). The Tarasa section with a total thickness of 250 m is measured along this valley. The section is mainly composed of dark green to green basic volcanics with rare breaks including pelagic rocks (red, very thin to thin-bedded cherts and gray to beige, thin to very thin-bedded limestones with occasional chert nodules) (Fig. 4). Only seven basic volcanic samples (Tar-5, 10, 11, 12, 14, 26, 28) collected from this section were proved to be least-altered and suitable for geochemical analyses. Six additional volcanic rock samples (Tar-29, 34, 36, 38, 40 and 41) were collected from eastern and western bank of Tarasa Creek (Fig. 3; Table 1). Two samples (Tar-20 and 21) taken from the associated pelagic rocks yielded determinable radiolarians indicating the late middle Carnian and latest Carnian/earliest Norian to early Norian ages. Therefore the depositional age of this section was accepted as Late Triassic (late middle Carnian to early Norian) (Uzuncimen et al., 2009; 2011; Tekin et al., 2010).

Both the Korun-1 and the Korun-2 sections lie at the northeast of Adiyaman, one to two km away from Korun (Fig. 5

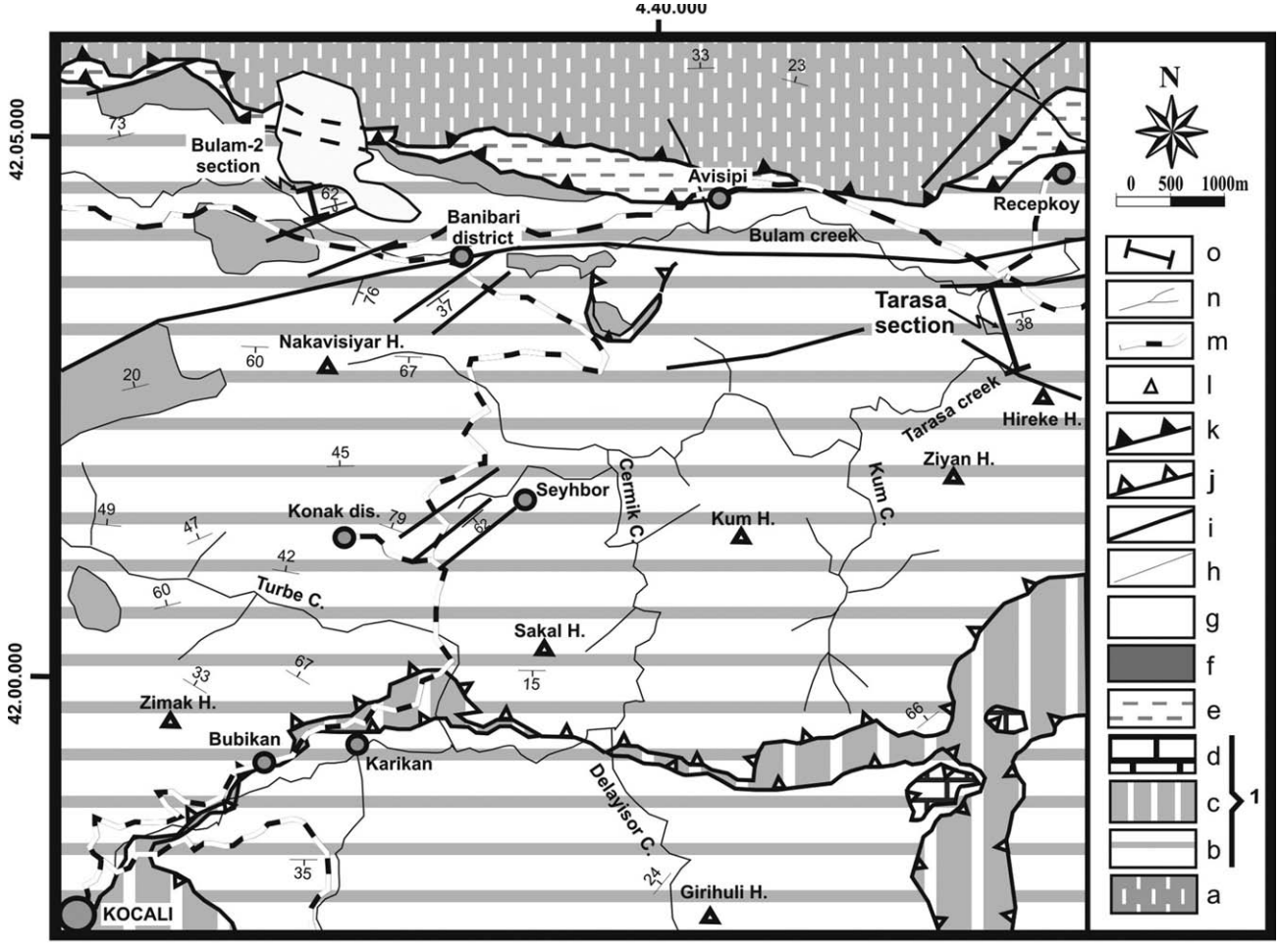

Fig. 3 - Geological map (revised after Sungurlu, 1973 and Perincek, 1979b) of the Adiyaman area with the localities of the Bulam-2 and the Tarasa sections. 1- The Kocali Complex of Triassic-Late Cretaceous age; a- Undifferentiated Bitlis-Poturge-Malatya Nappes; b- Undifferentiated Konak and the Tarasa Units; c- The Kale Ophiolite; d- The Cilo Limestones; e- The Maden Complex of Eocene age; f- Tertiary cover rock units; g- Recent deposits; h-Stratigraphic contact; i- Fault; j- Thrust; k- Upthrust; l- Main peaks; m- Main roads; n- Main drainage; o- Section location.

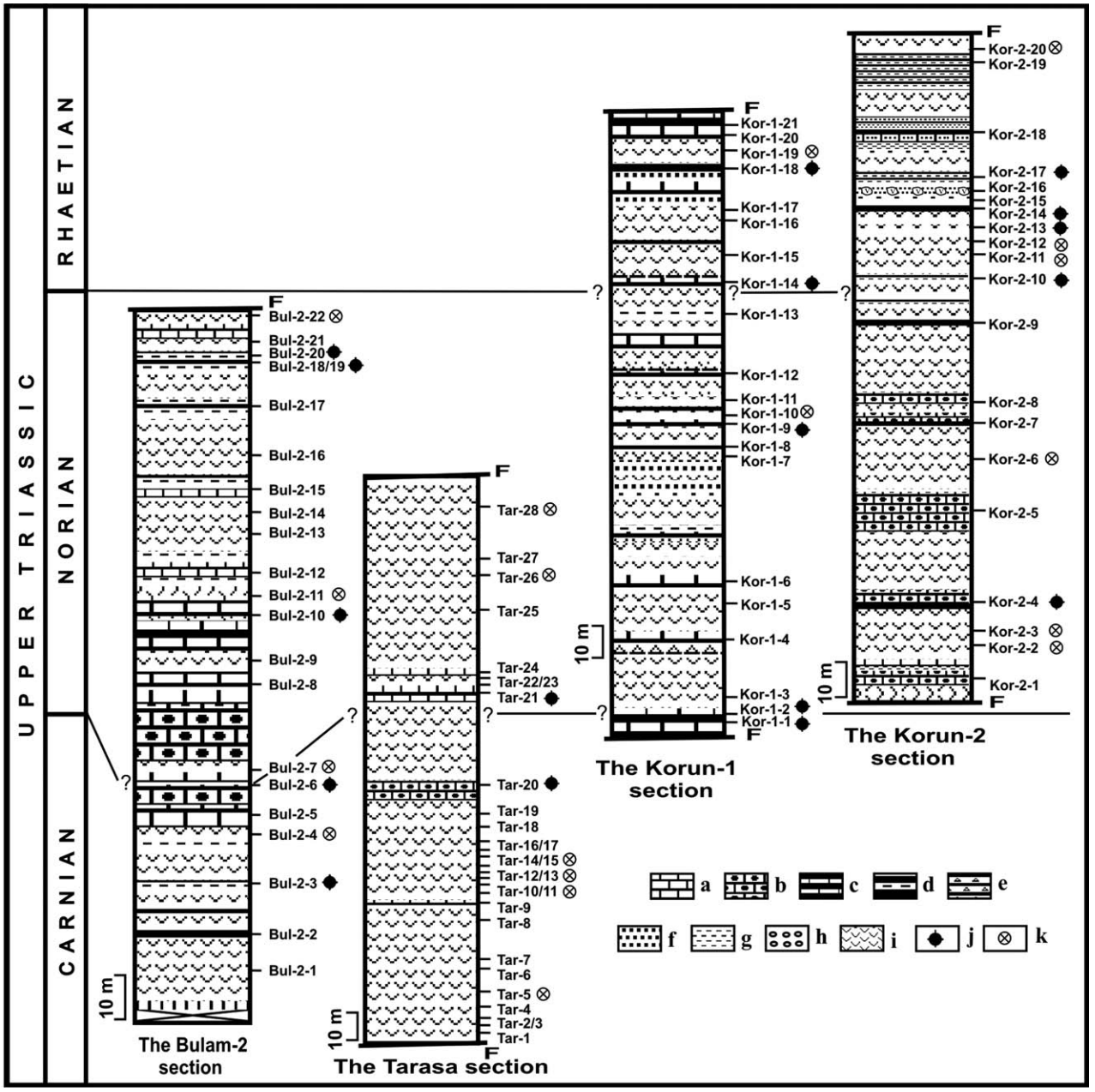

Fig. 4 - Correlation of the studied stratigraphic sections in this study. a- Limestones; b- Cherty limestones; c- Alternation of limestones and cherts; d- Alternation of mudstones and cherts; e- Calciturbidites; f- Sandstonse; g- Mudstones; h- Conglomerates; i- Basic volcanic rocks; j- Productive samples for Radiolaria determination; k- Samples for geochemical analyses from basic volcanics.

and Table 1). In this locality, different slices of the Kale Ophiolite and the Konak Unit of the Kocali Complex are overlain by Tertiary cover rocks (Fig. 5). The Korun-1 section with a total of 195 m thickness is composed mainly of green to dark green basic volcanic rocks with some thin to medium-bedded, gray to red limestone and chert interlayers (Fig. 4). The middle and upper parts of the section also include green to brown, medium to thick-bedded volcanogenic sandstones. Determinable radiolarian faunas were obtained from five of the samples (Kor-1-1, Kor-1-2, Kor-1-9, Kor-1-14 and Kor-1-18) in the section successively indicating middle late Carnian to early Norian (Kor-1-1), latest Carnian/earliest Norian to early Norian (Kor-1-2), latest Carnian/earliest Norian to late middle Norian (Kor-1-9), and Rhaetian (Kor-1-14 and Kor-1-18) ages. These data reveal that the depositional time span of the rock units in the Korun-1 section is middle late Carnian to Rhaetian (Uzuncimen et al., 2009; 2011; Tekin et al., 2010). Geochemistry of two relatively suitables basic volcanic rock samples (Kor-1-10 and Kor-1-19) is studied.

Lithological features of the Korun-2 section, situated at the NW of the Korun-1 section is very similar to the lithologies of the Korun-1 (Figs. 4, 5 and Table 1). A 200 m thick section in this locality is mainly composed of green to dark green basic volcanics (Fig. 4). Interlayers in these basic volcanics are composed of red, yellow, gray occasionally black, thin to medium-bedded cherts, gray to beige, thin to medium-bedded limestones with red to yellow chert nodules and red, thin-bedded silicified mudstones. Towards the upper

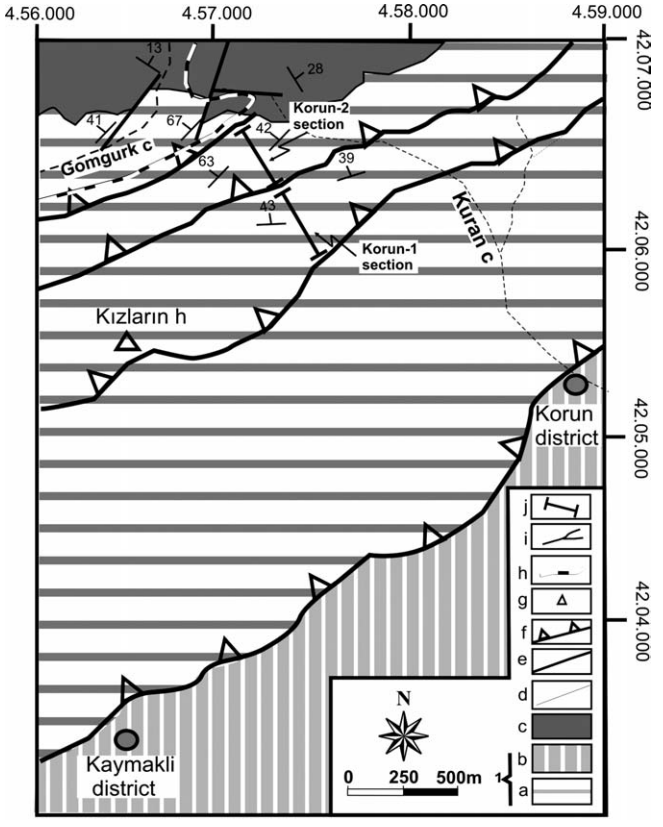

Fig. 5 - Geological map of northwest Adiyaman with the locations of the Korun-1 and the Korun-2 stratigraphic sections. 1- The Kocali Complex; a- The Konak Unit; b- The Kale Ophiolite; c- Tertiary cover rocks; d- Stratigraphic contact; e- Fault; f- Thrust; g- Main peaks; h- Main roads; i- Main drainage; j- Section place.

part of the section, green, thin to medium-bedded sandstone layers with volcanic clasts are also observed (Fig. 4). In this section, geochemical characteristics of six samples (Kor-2-2, Kor-2-3, Kor-2-6, Kor-2-11, Kor-2-12 and Kor-2-20) have been studied (Fig. 4). By determining radiolarian faunas of five samples, a late early Norian to early middle Norian (sample Kor-2-4) and Rhaetian (for samples Kor-2-10, Kor-2-13, Kor-2-14 and Kor-2-17) ages were assigned (Uzuncimen et al., 2009, 2011; Tekin et al., 2010) to this unit.

PETROGRAPHY

From four stratigraphic sections within the Kocali Complex (the Tarasa, the Bulam-2, the Korun-1 and the Korun-2), a total of twenty-eight least-altered samples were selected for the mineralogical and petrographical studies. Secondary minerals such as calcite, zeolite, chlorite filled the vesicles can be seen in these samples, indicative of low-grade alteration conditions.

From these, thirteen samples are from the Tarasa section. They exhibit hypocrystalline porphyritic texture with plagioclase, pyroxene ± olivine and amphibole phenocrysts and opaque microlites (Fig. 6A, B). Plagioclase phenocrysts are commonly subhedral but anhedral plagioclase phenocrysts are also observed. Pyroxene minerals are subhedral to anhedral and most of them are replaced by chlorite. Interstitial pyroxenes are dominated and typical ophitic textures are observed in these samples (Fig. 6A). Brownish amphibole crystals and olivine pseudomorphs are rarely found in some samples. Amphiboles seem to be formed by the alteration of pyroxene phenocrysts and olivine crystals are generally altered to serpentine. All these phenocrysts occur also as microphenocrysts settled in an intergranular to subophitic textured groundmass and the volcanic glass has been replaced by chlorite. In addition to these, sericite alteration occurs in most of the samples. They exhibit amygdaloidal texture filled with secondary minerals such as calcite, chlorite and zeolite (Fig. 6B).

Six samples obtained from the Bulam-2 section are porphyritic with tabular plagioclase and anhedral to interstitial pyroxene (Figs. 6C, D). Some of the samples display fine-grained aphyric texture. Small olivine phenocrysts occur in some samples. Sericite alteration is common and chlorite, calcite and zeolite minerals filled the vesicles of the samples. The groundmass is composed of the microlites of the same minerals.

A total of nine samples obtained from the Korun-1 and the Korun-2 sections display medium-grained aphyric textures and contain plagioclase, pyroxene ± olivine microphenocrysts (Fig. 6E, F). They exhibit porphyritic texture with generally altered phenocrysts. Pyroxene minerals are subhedral to anhedral in shape and more pleochroic than pyroxene minerals in sample from the Tarasa Unit. Typical intersertal and intergranular textures are encountered in all samples (Fig. 6F). All veins observed in the samples are filled by calcite and chlorite.

ANALYTICAL TECHNIQUES

Only fresh samples were collected systematically from study area and they are crushed in a carbide disc mill. Major, trace and rare earth element concentrations were determined at the ACME Analytical Laboratories, Vancouver, by using Inductively Coupled Plasma-Atomic Emission Spectrometry (ICP-AES) for major elements and Inductively Coupled Plasma-Mass Spectrometry (ICP-MS) for trace elements. Standards used for the analyses are CSC, DS-7, SO-18.

GEOCHEMICAL CHARACTERISTICS

Twenty-four samples obtained from four sections (the Tarasa, the Bulam-2, the Korun-1 and the Korun-2) within the Kocali Complex were analyzed in this study (Table 2). The alteration could interpret the observed variable and high loss of ignition (LOI) values. During the conditions of alteration and up to medium metamorphic grades, the high field strength elements (HFSE) are mostly immobile in comparison with large ion lithophile elements (LILE) (Winchester and Floyd, 1977; Rollinson, 1993). LILE are not considered to be indicative of the original composition of the basic volcanic rocks. For this reason, the discrimination diagrams of HFSE were mostly utilised. Samples from these sections can be examined into two groups, the Tarasa Unit and the Konak Unit, on the basis of their petrological and geochemical characteristics.

Group 1: E-MORB type samples from the Tarasa Unit

The samples plot in subalkaline basalts field on the Zr/TiO_2 vs Nb/Y diagram of Winchester and Floyd (1977)

Table 2 - Major, trace and rare earth element concentrations of representative Group-1 and Group-2 volcanic rocks.

	Tarasa Unit (E-MORB)												
Sample no.	**TAR-1-05**	**TAR-1-10**	**TAR-1-11**	**TAR-1-12**	**TAR-1-14**	**TAR-1-26**	**TAR-1-28**	**TAR-1-29**	**TAR-1-34**	**TAR-1-36**	**TAR-1-38**	**TAR-1-40**	**TAR-1-41**
SiO_2	47,51	47,33	47,27	44,87	45,59	47,02	45,52	45,92	46,56	47,55	44,78	47,25	47,82
TiO_2	1,07	1,20	1,15	1,17	1,32	1,71	1,18	1,25	1,39	1,77	1,10	1,53	1,56
Al_2O_3	16,12	15,38	14,80	16,19	16,66	15,69	16,57	16,86	16,07	14,58	16,09	15,64	14,93
Fe_2O_3	7,51	11,71	10,81	11,37	12,73	11,67	8,96	11,26	10,15	13,61	10,09	11,44	12,11
MnO	0,15	0,19	0,17	0,18	0,24	0,20	0,18	0,20	0,19	0,21	0,16	0,20	0,20
MgO	7,06	7,86	8,11	10,02	7,59	7,19	7,34	7,51	6,92	7,39	7,10	7,09	7,28
CaO	11,74	9,77	10,97	8,89	9,58	8,85	12,05	9,97	11,15	8,50	12,78	9,65	8,93
Na_2O	3,62	3,00	2,95	2,32	2,72	4,00	2,82	2,77	3,05	3,21	2,39	3,39	3,43
K_2O	0,71	0,54	0,35	0,78	0,48	0,30	0,43	0,77	0,81	0,37	0,96	0,37	0,45
P_2O_5	0,10	0,11	0,09	0,10	0,12	0,16	0,09	0,12	0,12	0,17	0,10	0,14	0,16
LOI(1050°C)	4,10	2,60	3,00	3,80	2,70	2,90	4,50	3,10	3,30	2,30	4,10	3,00	2,80
Total	99,79	99,75	99,76	99,74	99,74	99,76	99,76	99,78	99,78	99,75	99,77	99,75	99,76
Mg#	65,08	57,10	59,80	63,60	54,17	54,99	61,89	56,94	57,48	51,84	58,25	55,13	54,38
Co	66,2	51,0	58,5	48,7	57,5	54,6	83,1	52,1	104,4	52,8	56,1	52,9	47,7
Rb	10,4	7,1	4,3	11,1	6,6	3,7	7,8	12,8	8,2	3,6	12,8	4,3	5,0
Sr	325,0	450,6	269,2	316,4	360,3	279,6	352,2	172,2	155,9	310,6	369,8	357,7	371,9
Y	19,4	22,1	20,8	21,2	25,8	31,2	21,5	22,9	26,2	32,6	21,0	30,1	28,3
Zr	59,1	66,2	68,0	62,0	73,2	91,5	59,4	69,8	65,7	102,2	57,0	87,4	90,5
Hf	1,8	1,9	1,6	2,0	2,2	2,9	1,6	2,1	2,0	3,1	1,7	2,5	2,7
Ta	0,3	0,3	0,3	0,3	0,5	0,5	0,3	0,4	0,4	0,5	0,3	0,4	0,4
Nb	3,2	4,1	4,0	4,2	4,5	6,1	3,3	4,5	4,4	6,4	3,3	4,9	6,5
Ba	39	16	23	33	26	30	18	67	40	27	55	40	50
La	3,7	4,3	3,4	4,0	4,5	5,7	3,4	4,8	4,4	5,9	3,3	4,7	5,7
Ce	8,8	10,9	10,0	10,5	11,9	14,8	9,6	11,9	12,0	16,0	8,8	12,9	15,3
Pr	1,42	1,69	1,62	1,62	1,84	2,34	1,49	1,86	1,90	2,53	1,43	2,08	2,31
Nd	7,60	8,80	8,70	8,70	9,20	11,40	8,10	9,30	9,40	12,40	6,80	10,70	11,00
Sm	2,30	2,60	2,56	2,48	2,94	3,59	2,51	2,77	2,95	3,82	2,34	3,39	3,35
Eu	0,95	0,97	0,96	0,93	1,06	1,33	0,93	1,02	1,13	1,39	0,89	1,25	1,19
Gd	2,92	3,36	3,24	3,12	3,67	4,47	3,19	3,48	3,79	4,70	3,09	4,32	4,18
Tb	0,59	0,60	0,60	0,58	0,69	0,84	0,60	0,64	0,72	0,91	0,56	0,88	0,79
Dy	3,49	3,87	3,91	3,70	4,30	5,36	3,53	4,00	4,53	5,59	3,64	5,10	4,94
Ho	0,73	0,81	0,76	0,79	0,95	1,16	0,79	0,86	0,96	1,24	0,79	1,14	1,06
Er	2,14	2,39	2,29	2,19	2,70	3,28	2,16	2,47	2,76	3,62	2,23	3,27	3,10
Tm	0,31	0,35	0,38	0,33	0,42	0,50	0,34	0,38	0,43	0,55	0,34	0,50	0,46
Yb	1,90	2,33	2,27	2,09	2,74	3,25	2,19	2,42	2,72	3,56	2,20	3,08	2,95
Lu	0,28	0,33	0,34	0,31	0,39	0,45	0,31	0,35	0,40	0,52	0,32	0,46	0,44
Th	0,3	0,4	0,2	0,3	0,5	0,5	0,5	0,4	0,5	0,8	0,3	0,4	0,6
U	0,1	0,1	0,1	0,1	0,2	0,2	0,2	0,2	0,4	0,2	0,3	0,1	0,2

Table 2 (*continued*).

	Konak Unit (OIB)										
Sample no.	**KOR-1-10**	**KOR-1-19**	**KOR-2-02**	**KOR-2-03**	**KOR-2-06**	**KOR-2-11**	**KOR-2-12**	**KOR-2-20**	**BUL-2-07**	**BUL-2-11**	**BUL-2-22**
SiO_2	42.75	41.70	42.16	43.85	45.18	42.04	41.51	43.22	43.96	43.96	43.28
TiO_2	4.13	3.65	3.05	3.13	2.59	3.28	3.39	3.15	2.78	2.81	2.73
Al_2O_3	13.94	13.78	15.10	15.23	14.32	14.49	14.66	15.58	13.54	14.29	14.88
Fe_2O_3	16.61	16.10	14.37	13.33	13.16	15.38	17.70	14.74	13.57	13.07	13.69
MnO	0.15	0.19	0.14	0.12	0.18	0.24	0.18	0.10	0.12	0.14	0.28
MgO	6.85	6.73	4.61	6.23	8.30	7.86	8.31	5.62	8.34	7.45	7.89
CaO	4.91	8.07	9.07	8.33	8.99	6.78	4.75	6.09	8.02	9.46	9.20
Na_2O	2.49	2.37	2.48	2.63	2.69	2.43	2.52	2.55	1.97	2.22	2.78
K_2O	0.40	0.91	0.41	0.50	0.85	0.73	0.48	0.58	0.45	0.57	0.74
P_2O_5	1.25	0.91	0.43	0.46	0.35	0.57	0.54	0.47	0.46	0.42	0.42
LOI(1050°C)	6.20	5.30	7.90	5.90	3.00	5.90	5.60	7.60	6.50	5.30	3.80
Total	99.71	99.68	99.72	99.70	99.66	99.70	99.70	99.73	99.71	99.69	99.72
Mg#	44.99	45.32	38.88	48.10	55.57	50.33	48.21	43.05	54.93	53.06	53.33
Co	28.1	45.1	48.7	41.5	47.3	48.3	60.4	58.0	45.4	52.5	47.3
Rb	3.8	11.8	6.7	8.9	9.0	4.7	3.4	13.3	5.8	9.4	7.0
Sr	315.2	476.5	432.2	400.5	650.4	350.7	291.2	286.8	311.0	331.0	317.8
Y	46.6	41.8	32.3	31.8	25.8	23.9	21.9	27.6	27.1	28.7	21.3
Zr	228.5	217.9	222.6	223.8	157.0	124.6	120.6	203.5	164.8	193.1	99.8
Hf	6.3	6.0	6.1	6.3	4.6	3.3	3.7	6.0	4.7	5.2	3.0
Ta	2.2	2.5	2.3	2.2	1.6	1.2	1.2	2.1	1.6	1.9	0.9
Nb	36.8	38.1	36.6	37.3	24.0	20.6	20.0	33.8	25.7	30.9	13.6
Ba	257	245	156	169	248	222	175	121	106	176	219
La	36.9	36.0	27.5	28.3	20.0	18.9	18.0	24.7	21.5	23.8	12.5
Ce	87.5	82.2	61.3	62.1	44.9	44.6	42.6	54.3	49.0	53.4	30.1
Pr	12.32	11.40	8.17	8.22	6.15	6.32	6.00	7.14	6.61	7.23	4.28
Nd	54.70	50.40	34.70	33.80	26.80	29.50	27.90	31.20	29.70	32.30	20.50
Sm	11.45	10.52	7.37	7.35	5.81	6.44	5.99	6.38	6.44	6.80	4.85
Eu	4.06	3.23	2.34	2.37	1.89	2.51	2.35	2.17	2.13	2.21	1.78
Gd	10.95	9.91	7.00	7.02	5.58	6.10	5.53	6.18	6.17	6.47	4.79
Tb	1.68	1.54	1.14	1.15	0.91	0.94	0.88	1.02	0.99	1.09	0.79
Dy	9.06	8.25	6.21	6.15	4.85	4.95	4.67	5.56	5.40	5.74	4.27
Ho	1.73	1.59	1.19	1.19	0.96	0.92	0.86	1.03	1.00	1.13	0.80
Er	4.60	4.07	3.12	3.30	2.63	2.45	2.31	3.02	2.76	3.09	2.19
Tm	0.65	0.57	0.47	0.48	0.38	0.36	0.32	0.43	0.40	0.44	0.32
Yb	3.94	3.36	2.84	2.86	2.13	2.09	1.85	2.56	2.31	2.49	1.82
Lu	0.57	0.48	0.41	0.43	0.31	0.29	0.27	0.37	0.34	0.37	0.26
Th	3.0	3.3	3.2	3.0	2.0	1.6	1.5	2.5	2.1	2.3	1.1
U	0.8	0.8	0.9	0.8	0.6	0.4	0.6	0.8	0.7	0.7	0.3

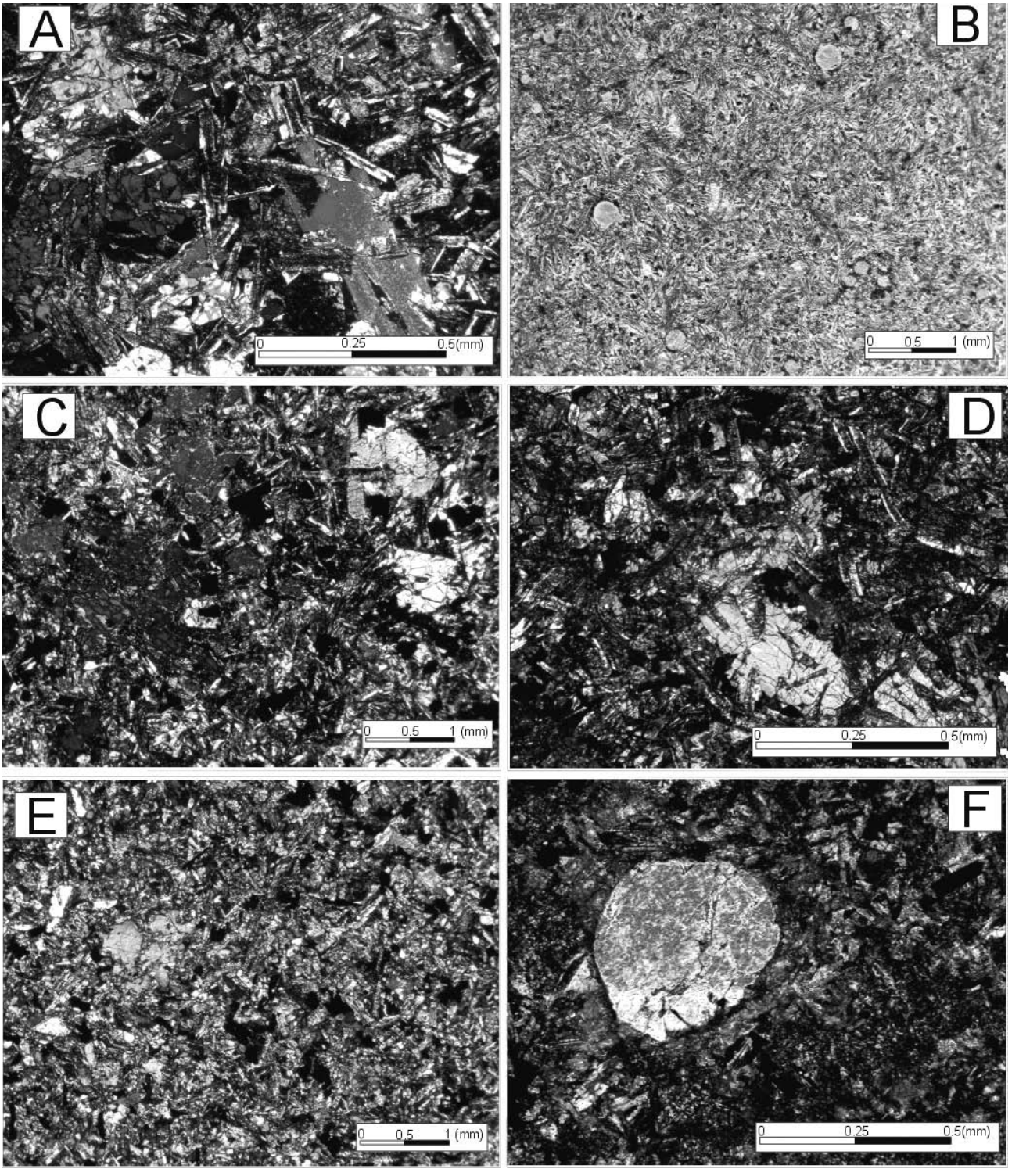

Fig. 6 - Photomicrographs from Group-1 and Group-2 volcanic rocks of the Kocali Complex: A) olivine, pyroxene and plagioclase phenocrysts and interstitial and ophitic textures observed in samples from Tarasa section; B) amygdaloidal texture filled with secondary minerals in sample from Tarasa section; C) tabular plagioclase and anhedral to interstitial pyroxene phenocrysts in sample from Bulam-2 section; D) pyroxene and plagioclase phenocrysts in samples from Bulam-2 section; E) intersertal and intergranular textures observed in sample from Korun-1 section; F) subhedral pyroxene phenocryst in sample from Korun-2 section.

(Fig. 7) with 44.78-47.82% SiO_2 content and the loss of ignition (LOI) values ranges between 2.30-4.50%. The subalkaline basaltic rocks are tholeiitic in character with low TiO_2 contents. Their Mg# [Mg/(Mg+Fe_2+)] range between 52 to 65. For comparing the samples from the Tarasa section with the volcanites of different tectonic environments, MORB and chondrite normalized multi-element diagrams are drawn (Fig. 8A1, A2). They have a pattern close to typical E-MORB pattern (Sun and McDonough, 1989) and high LILE contents with respect to the N-MORB composition. The LREE/HREE ratios are about 1 (La_N/Yb_N = 1.0-1.3) and REE concentrations exhibit almost flat patterns like typical N-MORB. However, they are 10x enriched. On tectonomagmatic discrimination diagrams the samples plot within the N-MORB field in Meschede (1986) (Fig. 9A) and MORB-field in Pearce and Norry (1979) (Fig. 9B) as well as Shervais (1982) (Fig. 9C) diagrams. Nevertheless, the observed pattern on Fig. 10A and B seems to be originated from an enriched MORB-like source and therefore the mixing of two different melts can be suggested. We choosed typical N-MORB and OIB-type melts compositions of Sun and McDonough (1989) as end-members and made the mixing modeling using the equations by Langmuir et al. (1978). All samples plotted on the mixing curve of two different melts (N-MORB and OIB-type melts) (Fig. 10A, B). Therefore, it is suggested that the volcanics from the Tarasa Unit were derived from the mixing of N-MORB and OIB-like mantle sources. The Ta/Yb vs Th/Yb diagram of Pearce (1983) is very useful for the discrimination of the mantle sources and determination of additional possible components like subduction and/or crustal contamination to the mantle (Fig. 11). The Tarasa group plot in the mantle array and have E-MORB source characteristics which have not been affected by any crustal components. If it had the opposite, this suggestion should be supported by the negative Nb, Ta anomalies however in Fig. 8 there is no negative anomalies in these elements.

Group 2: OIB-type samples from the Konak Unit

They are alkaline basalts with 41.51-45.18% SiO_2 content for samples from the Korun-1, the Korun-2 sections and 43.28-43.96% for the samples obtained from the Bulam-2 section according to the Zr/TiO_2 vs Nb/Y diagram by Winchester and Floyd (1977) (Fig. 7). Their LOI values range between 3.0-7.90% and 3.80-6.50%, respectively. Volcanic rock samples show patterns that resemble to the OIB-like source pattern from MORB and chondrite normalized multi-element diagrams (Fig. 8B1, B2). They contain high LILE, LREE, low HREE, Y and Yb contents and display positive Nb, Ta and Ti anomalies. They plot within the ocean island and within plate basalts on the discrimination diagrams (Pearce and Norry, 1979; Shervais, 1982) (Fig. 9A, B and C). The Mg# [Mg/(Mg+Fe_2+)] of samples from these three sections are lower 45 (Korun-1), 39-56 (Korun-2) and 50-55 (Bulam-2) than the Mg# of samples from the Tarasa section. All samples derived from the Tarasa and Konak Units in the Kocali Complex have lower Mg# values than primary magmas (≥ 67) (Gill, 1981), indicating that they underwent a certain degree of fractionation.

The Tarasa group samples are more depleted and have higher LILE/HFSE and lower LREE/HREE (La/Yb = 1.5-2.0) ratios than the Konak group samples (La/Yb= 7.0-10.7). These data also suggest that the parent magma of the latter group was more evolved than the Tarasa group volcanic rocks. The LILE and LREE concentrations could increase in the case of crustal involvement, in this case, negative anomalies should be observed in the elements like Nb, Ta and Ti. However it can be distinguishable from the diagrams (Fig. 8B1, B2) that these elements have higher concentrations of these elements, and it can be said that the crustal components do not play an important role in the genesis of these volcanic rocks. Concentrations of these elements could increase because of the small degrees of partial

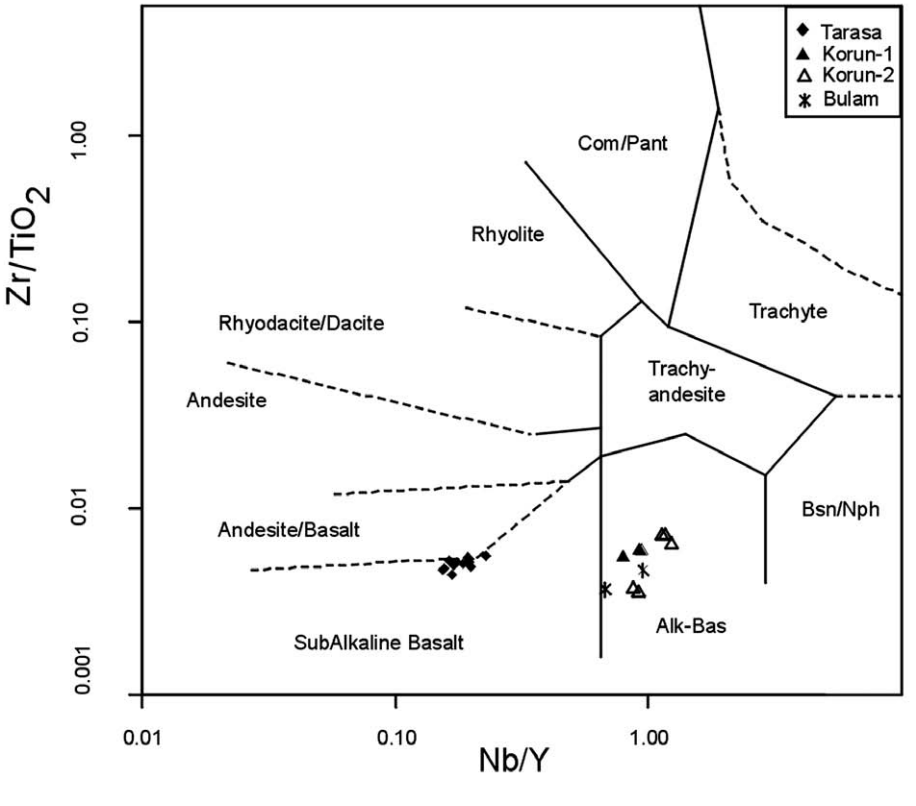

Fig. 7 - Zr/TiO_2 vs Nb/Y classification diagram (after Winchester and Floyd, 1977).

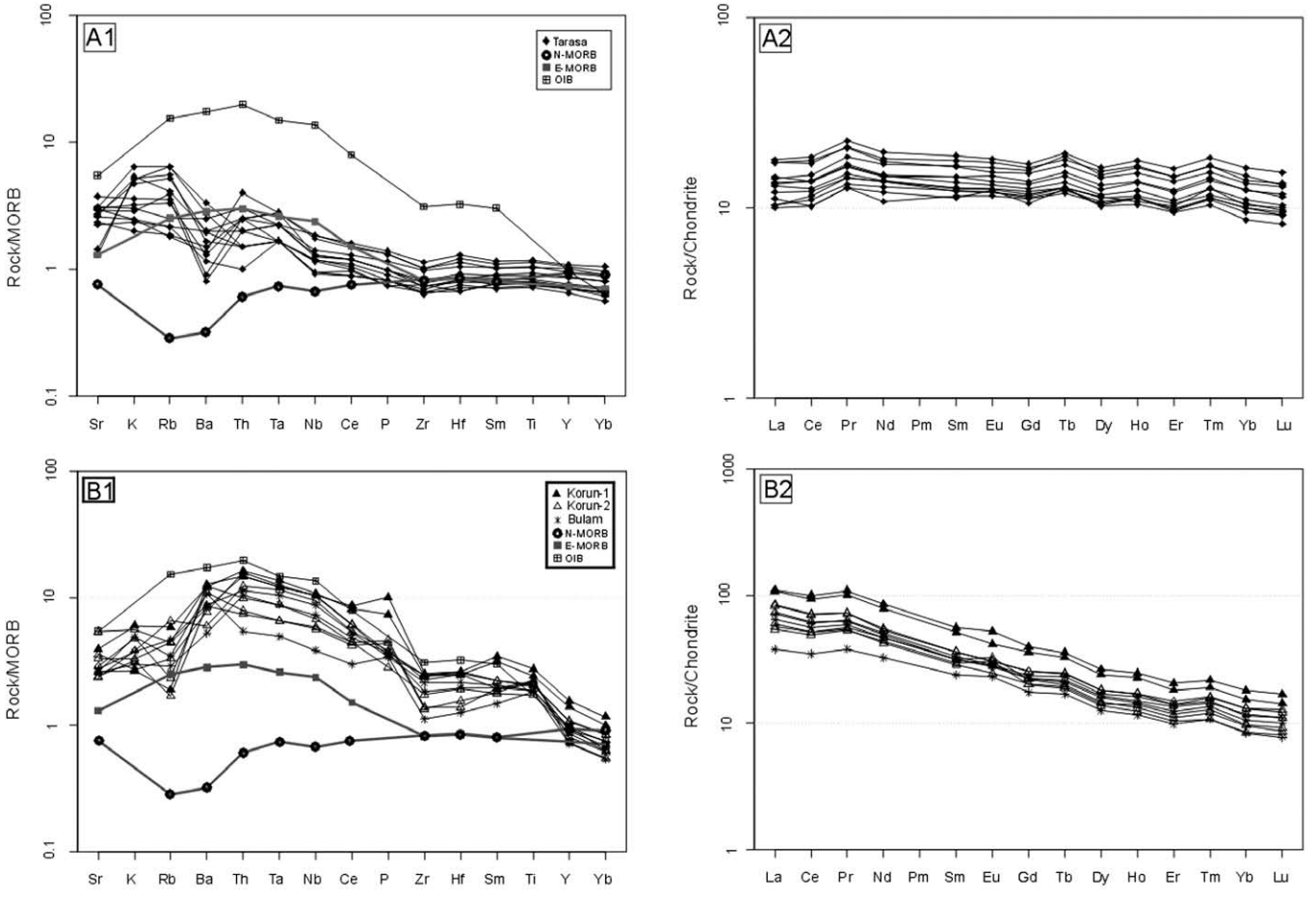

Fig. 8 - A1) MORB normalized (Pearce, 1983); A2) Chondrite normalized (Nakamura, 1974) multi-element diagram for the Group-1 volcanic rocks; B1) MORB normalized (Pearce, 1983); B2) Chondrite normalized (Nakamura, 1974) multi-element diagram for the Group-2 volcanic rocks.

melting, and their higher values suggest that residual garnet was present during partial melting. This reveals that the parent magma of the Bulam-2, the Korun-1 and the Korun-2 volcanic rocks are generated by the partial melting of a deep mantle source. The high La/Yb, Zr/Y ratios and the La/Nb ratio < 1 (La/Nb = 0.7-0.9 for this group) as proposed by De Paolo and Daley (2000) for deep mantle source, also supports their derivation from a deeper mantle source by partial melting process. On the Ta/Yb vs Th/Yb diagram of Pearce (1983), all the samples of this volcanic rocks group plot also within the mantle array field and have the composition of OIB-like source (Fig. 11). Based on these facts, it can be suggested that these rocks have all typical features of within plate alkaline basaltic rocks derived from a deeper OIB-like mantle source without any significant crustal contamination.

DISCUSSION AND CONCLUSION

Evolution of the Southern Tethyan oceanic basin have been well-documented by many authors and they indicate that it can be traced from the Hawasina basin to the east along Pichakun-Pindos through to the west (e.g. Ricou, 1971; Dumont et al., 1972; Ricou and Marcoux, 1980; Argyriadis et al., 1980; Robertson and Woodcock, 1982; Kazmin et al., 1986; Bechenec et al., 1988; Bernoulli et al., 1990). We think that the Kocali Complex in this system is an important missing link that has not been studied in detail yet in the geodynamic framework of the Southern Tethys.

In the previous studies (Uzuncimen et al., 2009; 2011; Tekin et al., 2010), the age of the volcanic sequences in this basin have been assigned to Late Triassic (middle Carnian to Rhaetian) based on the radiolarian determinations from the associated pelagic rock units. It is shown that the Kocali Complex actually contains two different types of Late Triassic volcanism: E-MORB-like mantle source generated by mixing of OIB and MORB-type melts (Group-1 volcanic rocks from the Tarasa Unit) and OIB-like (Group-2 volcanic rocks from the Konak Unit) mantle source.

The volcanic rocks of the Kocali Complex was previously studied by Bingöl (1994) and the subduction-related generation (arc volcanism) was suggested by him. He claimed that the volcanic rocks of this complex were the island arc products of Late Cretaceous time span. In general, the geochemical features such as high Ba/Nb, La/Nb, Th/Ta, Ba/Ta ratios and negative Nb, Ta, Ti anomalies in spider diagrams indicate a subduction related volcanism and/or effective crustal contamination process (Fitton et al., 1988; Hofmann, 1988; Wilson, 1989; Rudnick, 1995). However none of the samples from the Tarasa and the Konak Units in this study has these features. We think that this result arose due to misinterpretation of data. The Group-2 volcanic rocks are developed in a within-plate environment while the Group-1's are the products of enriched-MOR magmatism that have been likely generated by the interaction of OIB-type and MORB-type melts. None of the volcanic rocks of the Kocali

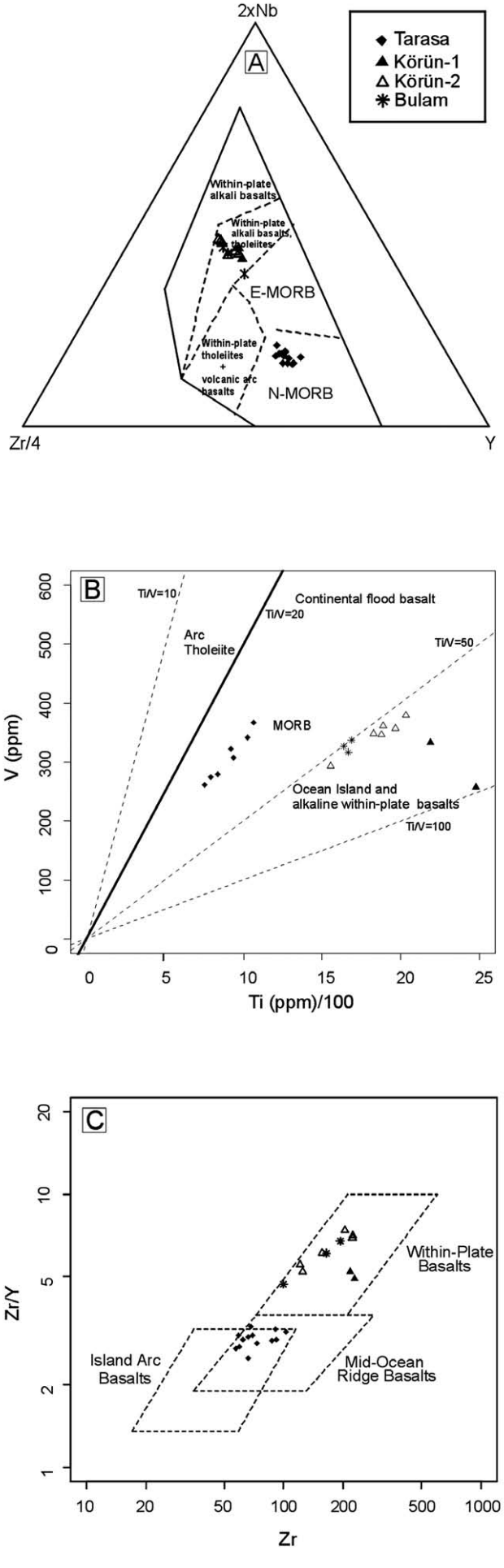

Fig. 9 - Tectonic discrimination diagrams; **A.** Nb-Zr-Y (after Meschede, 1986); **B.** Zr/Y-Zr (after Pearce and Norry, 1979); **C.** V-Ti/100 (after Shervais, 1982).

Complex was affected by crustal contamination and these data reveal that they are all developed in an oceanic environment. The presence of Radiolaria- and Bivalvia-bearing pelagic limestones, cherts interbedded within the basic volcanic rocks indicates also a deep marine basin (O'Dogherty et al., 2001). All these data emphasize that the Late Triassic volcanic rocks of the Kocali Complex developed probably in a rift zone instead of a subduction zone. Furthermore, none of the samples collected from the study area has N-MORB signatures. This suggests that the tholeiitic basalts from the Tarasa Unit displaying E-MORB characteristics and the alkaline basalts with typical OIB characteristics from the Konak Unit could be formed in a marginal oceanic basin away from the ocean ridge.

When volcanic rocks of the Late Triassic age in the Kocali Complex are compared the coeveal volcanic rocks in the adjacent areas of the same belt (e.g. Baer-Bassit region, NW Syria, the Mamonia Complex, SW Cyprus and the Antalya Nappes, SW Turkey), it is obvious that they have great similarities to each other. In detail, volcanic activities have been dated as Carnian to Norian in the Baer-Bassit Mélange, NW Syria (Al-Riyami et al., 2000; 2002; Al-Riyami and Robertson, 2002; Chan et al., 2007), Carnian-Norian in the Mamonia Complex (Lapierre et al., 2007) and middle to late Carnian in the Antalya Nappes, SW Turkey (Varol et al., 2007; Maury et al., 2008). Volcanic rocks in these regions have the characteristics of an enriched mantle source (OIB-like mantle source) and they are all alkaline basalts in character. Furthermore, the crustal contamination is not an important process in the formation of the volcanic rocks exposed in these regions (Al-Riyami and Robertson, 2002; Lapierre et al., 2007; Varol et al., 2007; Maury et al., 2008). The Mamonia Complex in SW Cyprus also includes depleted tholeiitic basalts, oceanic island tholeiites besides the alkaline basalts. The volcanic rocks of the Mamonia Complex were derived from a heterogeneous OIB-type mantle source according to Lapierre et al. (2007) however, the tholeiitic basalts originated from a MORB-like mantle erupted from the oceanic spreading centre according to Chan et al. (2008). With the exception of these MOR-type tholeiitic basalts, all the other volcanic rocks in these regions are the OIB-type products of a within-plate type tectonic setting (Al-Riyami et al., 2000; 2002; Al-Riyami and Robertson, 2002; Chan et al., 2007; Varol et al., 2007; Maury et al., 2008). Volcanic rocks of Tarasa Unit can be differentiated from the coeval volcanics exposed in adjacent areas by having a E-MORB characteristics.

Based on these facts, it can be concluded that volcanosedimentary sequences of the Kocali Complex are correlatable to the sequences in the Southern Tethyan Belt (e.g. the Baer-Bassit region in NW Syria, the Mamonia Complex in SW Cyprus and the Antalya Nappes in SW Turkey). When considering the geochemical data obtained from Late Triassic basic volcanics in the Kocali Complex and geochemical characteristics of the coeval volcanics of the adjacent units in the Southern Tethyan Belt, it can be suggested that rifting age of the Southern Tethyan Oceanic Basin in SE Anatolia is possibly earlier than early Late Triassic (middle Carnian time).

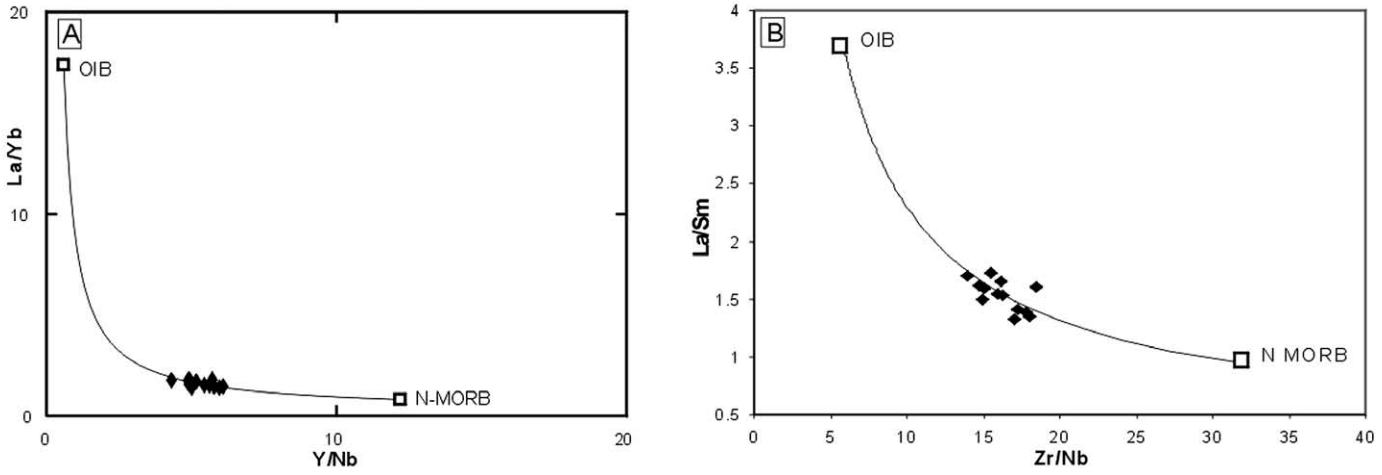

Fig. 10 - A) La/Yb vs Y/Nb; B) La/Sm vs Zr/Nb magma mixing modelling diagrams for Group-1 volcanic rocks (mixing curves formed after Langmuir et al. (1978) and the compositions of N-MORB and OIB are from Sun and Mc Donough (1989)).

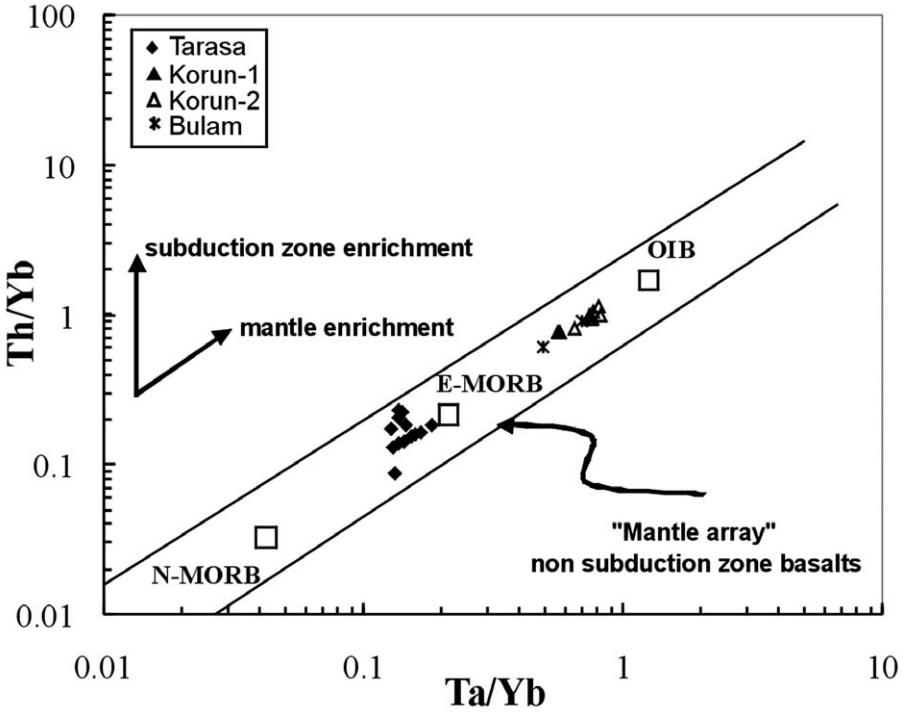

Fig. 11 - Th/Yb vs Ta/Yb diagram for volcanic rocks from the Kocali Complex (after Pearce, 1983).

ACKNOWLEDGEMENTS

The authors wish to thank Prof. Dr. Dogan Perincek and Mr. Metin Beyazpirinc for their kind contributions during the fieldwork. We are indepted to Turkish Scientific Council (Project No: 108Y001) for providing financial support. We are also grateful to T. Morishita and E. Saccani for their helpful comments.

REFERENCES

Argyriadis I., De Graciansky P., Marcoux J. and Ricou L.E., 1980. The opening of the Mesozoic Tethys between Eurasia and Arabia-Africa. Congr. Geol. Int. Colloq. C5. Mem. Bur. Rech. Geol. Min., 115: 199-214.

Al-Riyami K., Robertson A.H.F., Xenophontos C., Danelian T. and Dixon J.E., 2000. Mesozoic tectonic and sedimentary evolution of the Arabian continental margin in Baer-Bassit (NW Syria). In: J. Malpas et al. (Eds.), Proc. 3rd Intern. Conf. Geology of the Eastern Mediterranean, Nicosia, Cyprus, September 1998). Geol. Surv. Dept. Cyprus, p. 61-81.

Al-Riyami K., Danelian T. and Robertson A.H.F., 2002. Radiolarian biochronology of Mesozoic deep-water successions in NW Syria and Cyprus: implications for south-Tethyan evolution. Terra Nova, 14: 271-280.

Al-Riyami K.K. and Robertson A.H.F., 2002. Mesozoic sedimentary and magmatic evolution of the Arabian continental margin, northern Syria: evidince from Baer-Bassit Mélange. Geol. Mag., 139 (4): 395-420.

Bazzucchi P., Bertinelli A., Ciaripica G., Marcucci M., Passeri L., Rigo M. and Roghi G., 2005. The Triassic-Jurassic stratigraphic succession of Pignola (Lagonegro-Molise Basin, Southern

Apennines, Italy). Boll. Soc. Geol. It., 124: 143-153.
Bechenec F., Le Metour J., Rabu D., Villey M. and Beurrier M., 1988. The Hawasina Basin: A fragment of a starved passive continental margin, thrust over the Arabian Platform during obduction of the Sumail Nappe. Tectonophysics, 151: 323-343.
Bechenec F., Le Metour J., Rabu D., Grissac B., De Wever P., Beurrier M. and Villey M., 1990. The Hawasina Nappes: stratigraphy, palaeogeography and structural evolution of a fragment of the southern Tethyan passive continental margin. In: A.H.F. Robertson, M.P. Searle and A. Ries (Eds.), The geology and tectonics of the Oman Region. Geol. Soc. London Spec. Publ., 49: 213-223.
Bernoulli D. and Weissert H., 1987. The upper Hawasina nappes in the cenral Oman Mountains: stratigraphy, palinspastic and sequence of nappe emplacement. Geodin. Acta, 1 (1): 47-58.
Bernoulli D., Weissert H. and Blome C.D., 1990. Evolution of the Triassic Hawasina Basin, central Oman Mountains. In: A.H.F. Robertson, M.P. Searle and A. Ries (Eds.), The geology and tectonics of the Oman Region. Geol. Soc. London Spec. Publ., 49: 189-202.
Bertinelli A., Ciarapica G., De Zanche V., Marcucci M., Mietto P., Passeri L., Rigo M. and Roghi G., 2005. Stratigraphic evolution of the Triassic-Jurassic Sasso di Castalda succession (Lagonegro Basin, Southern Apennines, Italy). Boll. Soc. Geol. It., 124: 161-175.
Bingol A.F., 1994. The geochemistry and petrology of magmatic rocks from Kocali Complex, located within Çermik district (Diyarbakır, Southeast Turkey). Turk. J. Earth Sci., 3: 55-61. (in Turkish with English abstract).
Bragin N.Yu., 2007. Late Triassic Radiolarians of Southern Cyprus. Paleont. J., 41 (10): 951-1029.
Bragin N.Yu., Bragina L.G. and Krylov K.A., 2000. Albian-Cenomanian deposits of the Mamonia Complex, Southwestern Cyprus. In: I. Panayides, C. Xeenophontos and J. Malpas (Eds.), Proceed. 3rd Intern. Conf. Geology of the Eastern Mediterranean, p. 309-315.
Chan G.H.N., Malpas J., Xenophontos C. and Lo C.H., 2007. Timing of subduction zone metamorphism during the formation and emplacement of Troodos and Baer-Bassit ophiolites: insights from ^{40}Ar-^{39}Ar geochronology. Geol. Mag., 144: 797-810.
Chan G.H.N., Malpas J., Xenophontos C. and Lo C.H., 2008. Magmatism associated with Gondwanaland rifting and Neo-Tethyan oceanic basin development: evidence from the Mamonia Complex, SW Cyprus. J. Geol. Soc. London, 165: 699-709.
Danelian T. and Robertson A.H.F., 2001. Neotetyhyan evolution of eastern Greece (Pagondas Melange, Evia Island) inferred from radiolarian biostratigraphy and the geochemistry of associated extrusive rocks. Geol. Mag., 138 (3): 345-363.
Delaune-Mayère M., 1984. Evolution of a Mesozoic passive continental margin. Baer-Bassit (NW Syria). In: J.E. Dixon and A.H.F. Robertson (Eds), The geological evolution of the Eastern Mediterranean. Geol. Soc. London Spec. Publ., 17: 151-159.
De Paolo D.J. and Daley E.E., 2000. Neodymium isotopes in basalts of the southwest basin and range and lithospheric thinning during continental extension. Chem. Geol., 169: 157-185.
De Wever P., Bourdillon-De Grissac Ch. and Bechenec F., 1988. A Permian age from radiolarites of the Hawasina Nappes, Oman Mountains. Geology, 16: 912-994.
De Wever P., Bourdillon-de Grissac C. and Bechennec F., 1990. Permian to Cretaceous radiolarian biostratigraphic data from the Hawasina Complex, Oman Mountains. In: A.H.F. Robertson, M.P. Searle and A. Ries (Eds.), The geology and tectonics of the Oman Region. Geol. Soc. London Spec. Publ., 49: 225-238.
Dumont J.F., Gutnic M., Marcoux J., Monod O. and Poısson A. 1972. Le Trias des Taurides occidentales (Turquie). Definition du bassin pamphylien: Un nouveau domaine a ophiolithes a la marge externe de la chaine taurique. Zeitsch. Deutsch. Geol. Ges., 123: 385-409.
Elmas A. and Yilmaz Y., 2003. Development of an oblique subduction zone - Tectonic evolution of the Tethys Suture Zone in southeast Turkey. Intern. Geol. Rev., 45: 827-840.
Fitton J.G., James D., Kempton P.D., Ormerod D.S. and Leeman W.P., 1988. The role of lithospheric mantle in the generation of late Cenozoic basic magmas in the Western United States. J. Petrol., Spec. Issue, p. 331-349.
Fleury J.-J., 1980. Les zones de Gavrovo-Tripolitza et du Pinde-Olonos (Grece continentale et Peloponnèse du Nord). Evolution d'une plateforme et d'un bassin dans leur cadre alpin. Soc. Geol. Nord. Publ., 4.
Gharib F., 2009. Biostratigraphie des Radiolarites de Kermenshah (Iran). Ph. D. Thesis, Museum Nat. Ecole Doctorale, 338 pp. (unpublished).
Gharib F. and De Wever P., 2009. Mesozoic radiolarians from the Kermanshah Formation (Iran). The 12th Meet. Intern. Ass. Radiolarian Palaeontol., Abstr., p. 64-65.
Gill J.B., 1981. Orogenic andesites and plate tectonics, Springer Verlag, New York, 138 pp.
Goncuoglu M.C., Dirik K. and Kozlu H., 1997. General characteristics of pre-Alpine and Alpine Terranes in Turkey: Explanatory notes to the terrane map of Turkey. Ann. Géol. Pays Héllén., 37: 515-536.
Hofmann A.W., 1988. Chemical differentiation of the Earth: the relationship between mantle, continental crust and oceanic crust. Earth Planet. Sci. Lett., 90: 297-314.
Kazmin V., Ricou L.E. and Sbortshikov I.M., 1986. Structure and evolution of the passive margin of the eastern Tethys. Tectonophysics, 123: 153-179.
Langmuir C.H., Vocke R.D., Hanson G.N. and Hart S.R., 1978. A general mixing equation with applications to Icelandic basalts. Earth Planet. Sci. Lett., 37: 380-392.
Lapierre H., 1975. Les formations sedimentaires et eruptives des nappes de Mamonia et leurs relations avec le Masif du Troodos (Chypre occidentale). Mem. Soc. Géol. France, 123-131.
Lapierre H., Bosch D., Narros A., Mascle G.H., Tardy M. and Demant A., 2007. The Mamonia Complex (SW Cyprus) revisited: remnant of Late Triassic intra-oceanic volcanism along the Tethyan southwestern passive margin. Geol. Mag., 144: 1-19.
Lapierre H., Samper A., Bosch D., Maury R.C., Bechennec F., Cotten J., Demant A., Brunet P., Keller F. and Marcoux J., 2004. The Tethyan plume: geochemical diversity of Middle Permian basalts from the Oman rifted margin. Lithos, 74: 167-198.
Maury R.C., Bechennec F., Cotten J., Caroff M., Cordey F. and Marcoux J., 2003. Middle Permian plume-related magmatism of the Hawasina Nappes and the Arabian Platform: implications on the evolution of the Neotethyan margin in Oman. Tectonics, 22 (6): 1073.
Maury R.C., Lapierre H., Bosch D., Marcoux J., Krystyn L., Cotten J., Bussy F., Brunet P. and Senebier F., 2008. The alkaline intraplate volcanism of the Antalya nappes (Turkey): a Late Triassic remnant of the Neotethys. Bull. Soc. Géol. France, 179 (4): 397-410.
Meschede M., 1986. A method of discriminating between different types of mid-ocean ridge basalts and continental tholeiites with the Nb-Zr-Y diagram. Chem. Geol., 56: 207-218.
Moix P., Gorican S. and Marcoux J., 2009. First evidence of Campanian radiolarians in Turkey and implications for the tectonic setting of the Upper Antalya Nappes. Cretac. Res., 30: 952-960.
Nakamura N., 1974. Determination of REE, Ba, Fe, Mg, Na and K in carbonaceous and ordinary chondrites, Geochim. Cosmochim. Acta, 38: 757-773.
O'Dogherty L., Martin-Algarra A., Gursky H.J. and Aguado R., 2001. The Middle Jurassic radiolarites and pelagic limestones of the Nieves Unit (Rondaide Complex, Betic Cordillera): Basin starvation in a rifted marginal slope of the Western Tethys. Intern. J. Earth Sci., 90 (4): 831-846.
Okay A.I. and Tuysuz O., 1999. Tethyan sutures of northern Turkey. In. B. Durand, L. Jolivet, F. Horvath and M. Serrane (Eds), The Mediterranean basins: Tertiary extension within the Alpine Orogen. Geol. Soc. London Spec. Publ., 156: 475-515.
Pearce J.A., 1983. The role of subcontinental lithosphere in magma genesis destructive plate margins. In: C.J. Hawkesworth and M.J. Nory (Eds.), Continental basalt and mantle xenolits, p. 230-249.

Pearce J.A. and Norry M.J., 1979. Petrogenetic implications of Ti, Zr, Y, and Nb variations in volcanic rocks. Contr. Min. Petr., 69: 33-47.

Perincek D., 1978. Geological investigation and petroleum prospects of the region between Celikhan-Sincik-Kocali (city of Adiyaman). Ph.D. Thesis, Istanbul Univ., TPAO Report, 1250, 212 pp. (in Turkish, unpublished).

Perincek D., 1979a. Interrelation of the Arabian and Anatolian plates. Guidebook for excursion B, First Geol. Congr. Middle East. The Geol. Soc. Turkey, 34 pp.

Perincek D., 1979b. Geological investigation of the region between Celikhan-Sincik-Kocali (city of Adiyaman). TPAO Report, 1394, 30 pp. (in Turkish, unpublished).

Perincek D., 1990. Stratigraphy of the Hakkari province, southeast Turkey. Turk. Ass. Petrol. Geol. Bull., 2 (1): 21-68 (in Turkish with English abstract).

Ricou L.E., 1971. Le croissant ophiolitique peri-arabe, une ceinture des nappes mises en place au Crétacé Superieur. Rev. Géog. Phys. Géol. Dyn., 13: 327- 350.

Ricou L.E., 1976. Evolution structurale des Zagrides. La region-clef de Neyriz (Zagros Iranien). Mem. Soc. Géol. France, 125: 140.

Ricou L.E. and Marcoux J., 1980. Organisation générale et role structural des radiolarites et des ophiolites le long du système alpino-méditerranéen. Bull. Soc. Géol. France, 7: l-14.

Robertson A.H.F. and Woodcock N.H., 1979. Mamonia Complex, southwest Cyprus: the evolution and emplacement of a Mesozoic continental margin. Geol. Soc. Am. Bull., 90: 61-65.

Robertson A.H.F. and Woodcock N.A., 1982. Sedimentary history of the southwestern segment of the Mesozoic-Tertiary Antalya continental margin, south-western Turkey. Ecl. Geol. Helv., 75 (3): 517-562.

Robertson A.H.F., Parlak O., Rizaoglu T., Unlugenc U., Inan N., Tasli K. and Ustaomer T., 2007. Tectonic evolution of the South Tethyan Ocean: evidence from the Eastern Taurus Mountains (Elazig region, SE Turkey). In: A.C. Ries, R.W.H. Butler and R.H. Graham (Eds), Deformation of the continental crust. The legacy of Mike Coward. Geol. Soc. London Spec. Publ., 272: 231-270.

Robin C., Gorican S., Guillocheau F., Razin P., Dromart G. and Mosaffa H., 2010. Mesozoic deep-water carbonate deposits from the southern biostratigraphy, facies sedimentology and sequence stratigraphy Tethyan passive margin in Iran (Pichakun nappes, Neyriz area): biostratigraphy, facies sedimentology and sequence stratigraphy. Geol. Soc. London Spec. Publ., 330: 179-210.

Rollinson H.R., 1993. Using geochemical data: evaluation, presentation, interpretation. Longman Scient. Techn., John Wiley and Sons, New York, 352 pp.

Rudnick R.L., 1995. Making continental crust. Nature, 378: 571-578.

Senel M., 2002. 1/100.000 scale Turkish geological maps, Hakkari-M52 and M53 quadrangales. Publ. General Direct. Mineral Res. Explor., 22 pp. (in Turkish with English abstract).

Senel M., Dalkilic H., Gedik I., Serdaroglu M., Bolukbasi S., Metin S., Esenturk K., Bilgin A. Z., Uguz M.F., Korucu M. and Ozgul N., 1992. Geology of the region among Egirdir-Yenisarbademli-Gebiz ve Geris-Koprulu (Isparta-Antalya). General Direct. Mineral Res. and Explor., Rept. 9390, 559 pp. (in Turkish, unpublished).

Sengor A.M.C. and Kidd W.S.F., 1979. Post-collosional tectonics of the Turkish-Iranian plateau and comparision with Tibet. Tectonophysics, 55: 361-376.

Sengor A.M.C. and Yilmaz Y. 1981. Tethyan evolution of Turkey: a plate tectonic approach. Tectonophysics, 75: 181-241.

Shervais, M., 1982. Ti-V plots and the petrogenesis of modern and ophiolitic lavas. Earth Plan. Sci. Lett., 59: 101-118.

Sun S.S. and Mc Donough W.F., 1989. Chemical and isotopic systematics of oceanic basalts: implications for mantle composition and processes. In: A.D. Saunders and J. Norry (Eds.), Magmatism in the ocean basin. Geol. Soc. London Spec. Publ., 42: 313-345.

Sungurlu O., 1973. Geology of the region between Golbasi-Gerger, district-VI. TPAO Rept. 802, 30 pp. (in Turkish, unpublished).

Tekin U.K., 1999. Biostratigraphy and systematics of late Middle to late Triassic radiolarians from the Taurus Mountains and Ankara Region, Turkey. Geol.-Paläont. Mitt. Inns., 5: 297 pp.

Tekin U.K., 2002a. Lower Jurassic (Hettangian-Sinemurian) radiolarians from the Antalya Nappes, Central Taurides, Southern Turkey. Micropal., 48 (2): 177-205.

Tekin U. K., 2002b. Late Triassic (late Norian-Rhaetian) radiolarians from the Antalya Nappes, central Taurides, Southern Turkey. Riv. It. Paleont. Strat., 108 (3): 1-26.

Tekin U.K. and Yurtsever T.S., 2003. Upper Triassic (lower to middle Norian) radiolarians from Antalya Nappes, Antalya, SW Turkey. J. Micropal., 22 (2): 147-162.

Tekin U.K., Bedi Y., Perincek D., Beyazpirinc M., Varol E. and Uzuncimen S., 2010. Dating of the Kocali Complex (southeastern Turkey) by using radiolarian fauna and geochemical and petrographical properties of its volcanics. Final Report, TUBITAK Project no. ÇAYDAG 108Y001, 280 pp. (in Turkish, unpublished).

Uzuncimen S., Tekin U.K., Bedi Y., Perincek D., Beyazpirinc M., Varol E., Soycan H. and Ikizer A., 2009. First evidence of Upper Triassic radiolarian faunas from the volcanic-pelagic sequences of the Kocali complex, SE Turkey: Remarks on the correlation of this complex to the other units in the central and western Taurides. 12th Meeting Intern. Ass. Radiolarian Palaeont., Abstr., p. 181-183.

Uzuncimen S., Tekin U.K., Bedi Y., Perincek D., Varol E. and Soycan H., 2011. Discovery of the Late Triassic (middle Carnian-Rhaetian) radiolarians in the volcano-sedimentary sequences of the Kocali Complex, SE Turkey: Correlation with the other Tauride units. J. Ass. Earth Sci., 40: 180-200.

Varol E., Tekin U.K. and Temel A., 2007. Dating and geochemical properties of middle to late Carnian basalts from the Alakircay Nappe of the Antalya Nappes, SW Turkey: Implications for the evolution of southern branch of Neotethys. Ofioliti, 32 (2): 163-176.

Wilson M., 1989. Igneous petrogenesis. Unwin Hyman Ltd., London, 466 pp.

Winchester J.A. and Floyd P.A., 1977. Geochemical discrimination of different magma series and their differentiation products using immobile elements. Chem. Geol., 20: 325-343.

Yilmaz Y., 1993. New evidence and model on the evolution of the southeast Anatolian orogen. Geol. Soc. Am. Bull., 105: 251-271.

Yilmaz Y. and Yigitbas E., 1990. The different ophiolitic-metamorphic assemblages of the SE Anatolia and their significance in the geological evolution of the region. Proceed. 8 th Petrol. Congr., p. 128-140 (in Turkish with English abstract)

Yurtsever T.S, Tekin U.K. and Demirel I.H., 2003. First evidence of the Cenomanian/ Turonian Boundary Event (CTBE) in the Alakirçay Nappe of Antalya Nappes, SW Turkey. Cretac. Res., 24: 41-53.

Received, October 21, 2010
Accepted, April 28, 2011